Terrestrial laser scanning for 3D forest modelling and reflectance simulation through radiative transfer

Simone Vaccari[1], Kim Calders[2], Martin Herold[2],
Harm Bartholomeus[2] & Martin van Leeuwen[3]

[1] School of Geosciences, The University of Edinburgh, Edinburgh, EH9 3JN, Scotland, simone.vaccari@ed.ac.uk
[2] Laboratory of Geo-Information Science and Remote Sensing, Wageningen University, Wageningen, 6708PB, The Netherlands, kim.calders@wur.nl, martin.herold@wur.nl, harm.bartholomeus@wur.nl
[3] Forest Resources Management, University of British Columbia, Vancouver, V6T 1Z4, Canada, mvanleeu@interchange.ubc.ca

Paper Number: SL2013-004

Abstract

Forests cover more than one third of the world's land surface and play an important role in capturing solar energy into biomass and regulating climate. Active remote sensing sensors called light detection and ranging (LiDAR) describe forest structural attributes by measuring interceptions of emitted laser pulses with the canopy, while passive, spectral sensors provide for the estimation of leaf and canopy chemical properties. This study investigates the potential of integrating these datasets, which is typically achieved through radiative transfer modelling (RTM). The spatial distribution of crown constituents in the 3D space in combination with radiometric vegetation characteristics influences the radiation interception, emission and scattering by canopy elements. In this study, the Monte Carlo Ray Tracing (MCRT) RTM model *librat* is used with the purpose of simulating radiometric properties of a 3D-modeled forest based on spectral libraries that characterize bark, soil and leaf spectral signatures. Our findings confirm that TLS is a valid technique that provides an independent and reliable estimation of forest attributes compared to other techniques (ALS underestimates tree heights of 0.65 m compared to TLS and field-measured tree height is user biased). Preliminary reflectance simulations through RTM show that spectral information can be simulated from a virtual forest model, which should stimulate the interest of further research. The estimation of reflectance proprieties from 3D vegetation models combined with radiometric properties is promising and offers prospects for fusion of data from both optical and LiDAR sensors.

1. Introduction

Forested ecosystems cover almost one third of the world's land area (FAO 2001). Changes in forest degradation, deforestation and regrowth, impact overall forest biomass and its biophysical characteristics (Dobson *et al.* 1995). Aboveground biomass is often used as an indicator of the total amount of carbon sequestrated by forests (Waring and Running 2007), and as a result accurate and timely monitoring of forest resources is critical (Kauppi 2003) to understand the role of carbon cycle on global warming (Booth *et al.* 2012).
Remote Sensing (RS) allows the investigation of forest areas with different approaches. Optical "passive" sensors are mounted on airborne and spaceborne platforms and investigate how vegetation interacts with solar radiation through absorption, transmission and reflection. By analysing the spectral response of vegetation, different land cover classes can be defined (e.g. agriculture, forest, wetland, etc.). However, vegetation spectral signatures provide limited information about forest biomass proprieties, which can be estimated by analysing forest

structure and its geometric arrangement in the three-dimensional (3D) space. The importance of 3D information for carbon biomass estimation is therefore crucial (Hall *et al.* 2011).
Time of flight LiDAR is an active RS technique that consists of transmitting pulses towards the object investigated, which pulses are partially reflected back to the sensor according to the object's physical and biochemical proprieties (Gong *et al.* 2010). By analysing the travel time between each pulse transmission and reception, and assuming the speed of light, the distance of each point from the scanner can be obtained, deriving its location in the 3D space. LiDAR systems can be mounted on spaceborne platforms (e.g. ICESat), on airplanes (Airborne Laser Scanning, ALS) or can be used on the ground (Terrestrial Laser Scanning, TLS). With spaceborne and ALS systems, objects are viewed from above. In the case of TLS systems, the below-canopy position of the scanner favours the acquisition of 3D information of the vertical forest structure. Examples of 3D forest attributes that can be investigated from TLS data analysis include diameter at breast height (DBH), stem location and tree height (Tansey *et al.* 2009), foliage profiles (Lovell *et al.* 2003), canopy gap fraction (GF, Danson *et al.* 2007) and Leaf Area Index (LAI, Martens *et al.* 1993). The drawback of TLS data is the extent of the area being scanned, which is limited by the below-canopy position of the scanner. To benefit from the high level of detail from TLS data and the larger extent from ALS, the challenge is to combine the advantages of both techniques.
Passive and active sensors can be integrated through Radiative Transfer Modelling (RTM). RTM pursues to model the reflectance of target areas based on a set of vegetation parameters (LAI, chlorophyll, etc.) or the explicit 3D scene structure. In this study, the 3D RTM model *librat* is investigated, which uses the geometric forest arrangement retrieved from active sensors to simulate passive (Lewis 1999 and Disney *et al.* 2011). Reflectance values derived through RTM can potentially be used to better understand the reflectance values retrieved from satellite data.
This study is structured as follows: tree structural parameters are first estimated from different techniques and then a comparison is performed to assess TLS accuracy. Secondly, a 3D model of the study area is produced using ellipsoidal crowns. This 3D forest model is then used to simulate forest reflectance proprieties through RTM. Finally, preliminary results of simulated reflectance values are compared against satellite-retrieved reflectance values.

2. Method

2.1 Study area and data specifications

The area selected for this study is located near the Loobos forest flux tower site (De Hoge Veluwe National Park, the Netherlands). The dominant forest species is Scots Pine (*Pinus sylvestris*) with sparse understory. This research was based on the analysis of a 25m × 25m plot which centre coordinate was x = 179376.5m, y = 464318.5m in the Dutch National coordinate system RD-New (Rijksdriehoeksmeting).
Terrestrial LiDAR data was collected in September 2011 with an RIEGL VZ-400 terrestrial laser scanner, with a zenith and azimuth resolution of 1.05mrad and beam divergence of 0.3 mrad. Data was acquired within the zenith range 30° - 130° and full azimuth. Nine scans were acquired at nine respective locations, which were chosen according to a 25m × 25m regular square sampling pattern. The nine scan locations were then co-registered to each other using reflective reference targets set up in the field, and a 25m × 25m area located in the centre of the plot was selected. TLS data was saved into the national RD-New coordinate systems.
Two airborne LiDAR datasets were also acquired at the site: the Actueel Hoogtebestand Nederland (Actual Height model of the Netherlands, AHN), which has a point density of 9 pts./m^2, and the LiDAR dataset provided by the Natural Environment Research Council (NERC), characterized by a point density of 10 pts./m^2. Both datasets were acquired in 2010 and re-projected into RD-New coordinate system in order to match the TLS dataset.
Hemispherical photographs were acquired using a Nikon Coolpix 8700 camera, fitted with an

FC-E9 Fisheye lens with 180° field of view. Like the TLS sampling-scheme, nine photos were taken at their respective scan location.
Optical imagery was acquired in September 2011 from the *Landsat Thematic Mapper 5* satellite, which was downloaded from the online Landsat application (http://glovis.usgs.gov/).

2.2 Forest 3D parameters retrieval

The 3D forest model was based on specific attributes that characterized the forest spatial arrangement. These include tree location, DBH, tree height, crown basal height, crown width and LAI.
The location of the trees within the study area was retrieved with two different approaches. In the first approach a 0.5 m resolution Canopy Model (CM), determined by subtracting the Digital Elevation Model (DEM) from the top of the canopy (TOC) surface, was investigated (Stereńczak and Zásada 2011). The location of the tree tops and their correspondent heights were extracted by investigating the CM local maxima using a neighbourhood filter of 1.5 m. In the second approach, from TLS data only, the location of the trees was obtained through the DBH analysis, which consists of estimating the stem diameter measure at the specific height of 1.3 m. To identify tree stems, a cross-section, 6 cm thick, of the TLS dataset was applied at 1.3 m height (1.27 m - 1.33 m, Tansey *et al.* 2009). For each tree, the stem circumference was iteratively determined through a circle fitting algorithm (Tansey *et al.* 2009): its centre and diameter represent tree location and DBH, respectively. The spatial distance between each location retrieved from CMs and the respective location obtained from DBH analysis was subsequently computed to compare the performance of the two approaches.
The Crown Basal Height (CBH) parameter refers to the height at which the crown starts, therefore the foliage profile of each tree (the foliage density distribution as a function of height) was analysed from the TLS. The Crown Width (CW) parameter refers to the projected (x, y) extent of the crown on the ground. To obtain CW values for individual trees, the morphology of the CM raster retrieved from TLS data was analysed. The CW values were retrieved by centring a circle in each tree location and iteratively increasing its radius until the percentage of ground cells was greater than a specified threshold, which condition indicated the crown extent.
LAI values were extracted from HP data over the zenith range 0° – 60°. Based on literature, it was assumed that the zenith angle that is least affected by multiple scattering of radiation for LAI estimation is 57.5° (Wilson 1963). The foliage within the canopy was assumed to be randomly distributed (unitary clumping index, Leblanc and Chen 2001). LAI values were computed for each of the nine hemispherical photos, and averaged to obtain the global LAI.
The retrieved parameters described the 3D structure of each tree located in the study forest. Tree crowns were modelled as ellipsoids and tree stems as cylinders, which dimensions were mathematically derived from the retrieved parameters. Tree crowns were populated by leaves determined by the parameter Disk Size Leaf, with a radius of 0.01 m. (Calders *et al.* 2013). Finally, each individual tree was translated in the 3D space according to its specific tree location.

2.3 Optical imagery

The Landsat imagery was re-projected into local RD-New coordinate system to align the satellite image with the LiDAR datasets. To correct the image from the atmospheric influence, radiometric correction was subsequently applied with the ATCOR software, which is a semi-empirical correction method that reduces the atmospheric effect by using specific illumination parameters (e.g. acquisition day, solar zenith angle, ground elevation, aerosol particles and visibility) (Richter 2003). The band-specific reflectance values of the study-area pixel and its surrounding eight pixels were subsequently averaged and used for validation.

2.4 Radiative Transfer Modelling

The foliage arrangement within canopies and the 3D geometry of a forest area influences the radiation interception, emission and scattering by canopy elements. Lewis (1999) presents a RT model called *librat*. The Monte Carlo Ray Tracing (MCRT) algorithm is the basis of the *librat* model, which models the reflectance by following the interactions of the radiation propagating through the constructed 3D scene by testing its scattering proprieties (Disney *et al.* 2000, 2011). The model *librat* simulates radiance values based on a 3D structural input and spectral libraries that characterize the scene elements.
To simulate the canopy reflectance, four main elements were involved (Disney *et al.* 2000). First, the 3D characteristic structure of the forest was reproduced according to the biophysical forest attributes. Secondly, the computational parameters of the MCRT simulation were specified. The third phase consisted of investigating the illumination conditions and the last phase analysed the specifications and characteristics of the simulated-sensor image.
In this study, only a single RTM simulation was undertaken based on solar- and sensor-specific angles (azimuth and zenith). This simulation provides an initial demonstration of the potential integration of active and passive RS systems with RTM. Future research into more detailed simulations, under different scenarios, are ongoing and will be described in later papers.

3. Result

3.1 3D parameter analysis

Tree locations extracted from CM analysis were compared with locations extracted from DBH analysis, which was used as reference. Twenty-four trees were estimated from both approaches. Four of them were only detected from DBH analysis and four other trees were retrieved from CM analysis only. When comparing the distances between respective tree locations, the largest highest difference occurred between the TLS CM-retrieved locations, which differed from the DBH-retrieved locations with an average distance of 2.09 m and standard deviation of 0.82 m.
The TLS-retrieved DBH estimates were compared with the field-measured DBH values (R^2 = 0.95), indicating the TLS is a reliable technique to derive DBH.
When tree heights derived from CM of the three LiDAR dataset were compared with each other, an $R^2 > 0.96$ was found in all cases, denoting a good agreement in height estimation from the LiDAR techniques. However, both ALS datasets were observed to underestimate tree heights with 0.65 m on average when compared to the TLS dataset. Comparing the CM-retrieved tree heights with the field-measured tree heights showed a mean absolute residual of 1.70 m for both ALS datasets and a mean absolute residual of 1.83 m for the TLS data set.
The analysis of individual tree crown dimensions included the crown basal height (CBH) and the crown width (CW). Foliage profiles were investigated to compute CBH values, which were compared with field-measured CBH values, showing a mean absolute residual of 1.88 m. The CW parameter was retrieved by analysing the TLS-derived CM, with the assumption that the projection of the tree crowns on the ground had a circular shape and a mean absolute residual of 1.54 m was found compared with field measurements.
An overall LAI value of 1.42 was obtained by averaging the nine LAI values derived from the hemispherical photos. Individual tree LAI values were then computed by distributing the LAI to individual trees based on the crown volume distribution. The final 3D forest model produced by retrieving 3D structural parameters is shown in Figure 1.

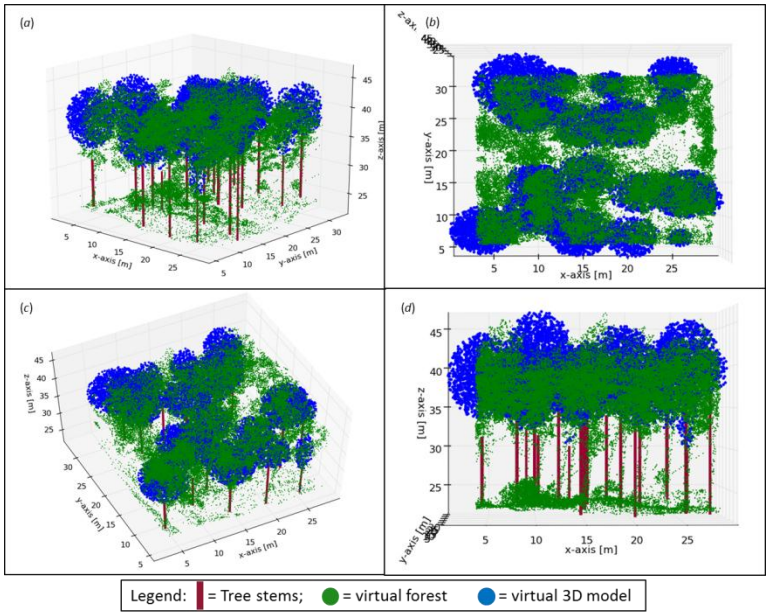

Figure 1: Snapshots of the created 3D virtual forest (in blue) together with the TLS pointcloud data (in green). The 3D scene is displayed at isometric view ((a) and (c)), from the top (b) and with profile-view (d).

3.2 Reflectance retrieval: Optical imagery and radiative transfer modelling comparison

The spectral profiles retrieved from the Landsat image and simulated through RTM are displayed in Table 1. The satellite-retrieved reflectance reflects the common vegetative spectral signatures, with low reflectance in the visible region (0.4µm– 0.7µm) due to the chlorophyll absorption features and high reflectance in the near infrared (0.7µm – 1.3µm) due to high reflective proprieties of vegetation leaves structure. Reflectance then decreases in the longer shortwave infrared wavelengths (1650nm and 2220nm) due to water absorption. The preliminary results for reflectance simulation are overall comparable to the satellite-derived reflectance, except for the NIR band where is observed a much higher value compared to the simulated one. The correlation between the two spectral signatures reported an R^2 of 53.42%.

Table 1: Reflectance values retrieved from Landsat and through RTM, ranging between 0 and 100.

	Wavelength [nm]					
	Blue	Green	Red	NIR	MIR 1	MIR 2
	490	560	660	830	1650	2220
Landsat	0,55	2,77	2,58	20,55	8,65	4,26
RTM simulation	1,07	1,65	1,43	5,95	6,74	4,81

4. Discussion

4.1. 3D parameters retrieval

Tree location determination was carried out with two approaches: from each tree tip through CM analysis and from each tree base through DBH analysis. The latter approach provided better estimation of tree location as trees within the forest were observed to have a leaning structure therefore the location of their tree tops projected on the ground was misplaced (2.09 m on

average). Additionally, trees identification from CM analysis was somewhat biased by the CM parameters settings used to create the CM raster, therefore tree location retrieved from DBH analysis was considered as the best estimation. Regarding the DBH measurements, TLS-derived estimates were observed to be highly correlated with field measurements (R^2 = 0.95).
Comparing tree heights estimated from TLS and ALS data, it was observed that ALS technique tends to underestimate tree heights of about 0.65 m compared to TLS estimates, which is similar to results found by Jung *et al.*, (2011), Faridhouseini *et al.* (2011) and in contradiction with Hilker *et al.* (2012) and Chasmer *et al.* (2006). The high beam resolution of the TLS scanner allows the laser pulse to penetrate deeper through the canopy, eventually reaching the top of the trees, whereas it may be missed by small-footprint ALS (Figure 2).

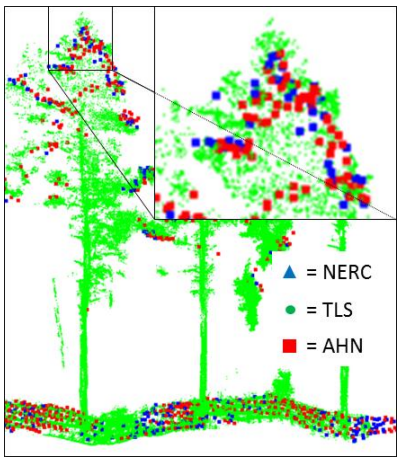

Figure 2: ALS underestimates tree heights compared to TLS.

Tree height and crown dimensions (CBH and CW) manually measured *in-situ* were characterized by uncertainty and user-bias. This is most likely the reason for the larger mean absolute residuals between TLS-retrieved and field-measured tree height (1.83 m), CBH (1.88 m) and CW (1.54 m).
The LAI value of the study area was derived from HP analysis and specific mathematical operations were subsequently used to compute tree-specific LAI values. Alternatively, LAI estimates could also be empirically retrieved from TLS data through the canopy GF analysis (Weiss *et al.* 2004). Relationships between TLS-derived and HP-derived GF values could additionally be used to decrease bias introduced by TLS systems (Vaccari *et al.* 2013). The LAI parameter obtained from TLS data can consequently be better estimated.
Methods presented in this study, provide for a high level of automation in modelling 3D forest models from TLS data. While the techniques are highly reproducible, the reconstruction results are highly dependent on assumptions and specific input parameters chosen around structural attributes such as leaf angle inclination distribution and foliage clumping. This should stimulate and address future research to further investigate the influence of each forest parameter on the obtained 3D model.

4.2. Reflectance comparison

The reflectance profile simulated through 3D RTM resembled vegetation spectral properties, with low reflectance in the visible part of the spectrum and higher values in the infrared region. However, a much higher value was expected in the NIR region due to high reflective proprieties of vegetation leaves structure. The reasons of this outcome are likely to be associated to the RTM parameters used and the 3D model created, and further research should test alternatives for improving results. Specifically, the 3D model created did not consider forest understory and therefore lacked of vegetative information associated with bushes and shrubs. In this

preliminary simulation results, a by pure bare soil, which has a low spectral response in the NIR, was used. Furthermore, by increasing the disk size leaf parameter, the vegetation reflectance is expected to increase. An additional forest propriety that could increase forest reflectance is the foliage clumping which, if modelled, increases the forest LAI and therefore its reflectance (Leblanc and Chen 2001).

5. Conclusion

In this study the potential of TLS in forestry was analysed to estimate individual tree structural attributes. These include includes tree location, tree heights, diameters at breast height, crown basal height, crown width and leaf area index. Results confirm that TLS has advantages compared to ALS data and field measurements for making a 3D forest model. RTM was subsequently used in order to simulate reflective proprieties of the study forest. Preliminary results show that spectral information can be simulated reasonably from a 3D forest model. Potential improvements are expected with increasing the 3D model complexity, including the topography and forest understory. The estimation of reflectance proprieties from 3D information combined with spectral signatures, rather than common techniques based on optical 2D data, is therefore achievable and offers promising prospective for fusion of data from both optical and LiDAR sensors.

References

Booth, B. B. B., Jones, C. D., Collins, M., Totterdell, I. J., Cox, P. M., Sitch, S., Huntingford, C., Betts, R. A., Harris, G. R. & Lloyd, J., 2012. High sensitivity of future global warming to land carbon cycle processes. *Environmental Research Letters,* 7.

Calders, K., Lewis, P., Disney, M., Verbesselt, J. and Herold, M., 2013. Investigating assumptions of crown archetypes for modelling LiDAR returns. *Remote Sensing of Environment,* 134, 39-49.

Chasmer, L., Hopkinson, C. and Reitz, P., 2006. Investigating laser pulse penetration through a conifer canopy by integrating airborne and terrestrial lidar. *Canadian Journal of Remote Sensing,* 32**,** 116-125.

Danson, F. M., Hetherington, D., Morsdorf, F., Koetz, B. and Allgöwer, B., 2007. Forest canopy gap fraction from terrestrial laser scanning. *IEEE Geoscience and Remote Sensing Letters,* 4, 157-160.

Disney, M. I., Lewis, P., Gomez-Dans, J., Roy, D., Wooster, M. J. & Lajas, D., 2011. 3D radiative transfer modelling of fire impacts on a two-layer savanna system. *Remote Sensing of Environment,* 115**,** 1866-1881.

Disney, M. I., Lewis, P. and North, P. R. J., 2000. Monte Carlo ray tracing in optical canopy reflectance modelling. *Remote Sensing Reviews,* 18**,** 163-196.

Dobson, C. M., Ulaby, F. T., Pierce, L. E., Sharik, T. L., Bergen, K. M., Kellndorfer, J., Kendra, J. R., Li, E., Lin, Y. C., Nashashibi, A., Sarabandi, K. and Siqueira, P., 1995. Estimation of forest biophysical characteristics in northern Michigan with SIR-C/X-SAR. *IEEE Transactions on Geoscience and Remote Sensing,* 33**,** 877-895.

FAO., 2001. Global forest resources assessment 2000. Main report. Food and Agriculture Organization of the United Nations (FAO). FAO Forestry Paper 140. Rome. 479 p.

Faridhouseini, A., Mianabadi, A., Bannayan, M. and Alizadeh, A., 2011. Lidar remote sensing for forestry and terrestrial applications. *International Journal of Applied Environmental Sciences,* 6**,** 103-118.

Gong, X., Wei, D. and Zhou, G., 2010. Extracting trees and structure parameters via integration of LiDAR data and ground imagery. International Geoscience and Remote Sensing Symposium (IGARSS), Honolulu, HI. 2703-2706.

Hall, F. G., Bergen, K., Blair, J. B., Dubayah, R., Houghton, R., Hurtt, G., Kellndorfer, J.,

Lefsky, M., Ranson, J., Saatchi, S., Shugart, H. H. and Wickland, D., 2011. Characterizing 3D vegetation structure from space: Mission requirements. *Remote Sensing of Environment,* 115**,** 2753-2775.

Hilker, T., Coops, N. C., Newnham, G. J., Van Leeuwen, M., Wulder, M. A., Stewart, J. And Culvenor, D. S., 2012. Comparison of terrestrial and airborne LiDAR in describing stand structure of a thinned lodgepole pine forest. *Journal of Forestry,* 110**,** 97-104.

Jung, S. E., Kwak, D. A., Park, T., Lee, W. K. and Yoo, S., 2011. Estimating crown variables of individual trees using airborne and terrestrial laser scanners. *Remote Sensing,* 3**,** 2346-2363.

Kauppi, P. E., 2003. New, low estimate for carbon stock in global forest vegetation based on inventory data. *Silva Fennica,* 37**,** 451-457.

Leblanc, S. G. and Chen, J. M., 2001. A practical scheme for correcting multiple scattering effects on optical LAI measurements. *Agricultural and Forest Meteorology,* 110**,** 125-139.

Lewis, P., 1999. Three-dimensional plant modelling for remote sensing simulation studies using the Botanical Plant Modelling System. *Agronomie,* 19**,** 185-210.

Lovell, J. L., Jupp, D. L. B., Culvenor, D. S. and Coops, N. C., 2003. Using airborne and ground-based ranging lidar to measure canopy structure in Australian forests. *Canadian Journal of Remote Sensing,* 29**,** 607-622.

Martens, S. N., Ustin, S. L. and Rousseau, R. A., 1993. Estimation of tree canopy leaf area index by gap fraction analysis. Forest Ecology and Management, 61, 91-108.

Richter, R., 2003. Status of Model ATCOR4 on Atmospheric / Topographic Correction For Airborne Hyperspectral Imagery. Presented at the 3rd EARSeL Workshop on Imaging Spectroscopy, Herrsching, 13-16 May 2003.

Stereńczak, K. and Zásada, M., 2011. Accuracy of tree height estimation based on LIDAR data analysis. *Folia Forestalia Polonica, Series A,* 53**,** 123-129.

Tansey, K., Selmes, N., Anstee, A., Tate, N. J. and DENNISS, A., 2009. Estimating tree and stand variables in a Corsican Pine woodland from terrestrial laser scanner data. *International Journal of Remote Sensing,* 30**,** 5195-5209.

Vaccari, S., Van Leeuwen, M., Calders, K., Coops, N. and Herold, M., 2013. Bias in LiDAR-based canopy gap fraction estimates. *Remote Sensing Letters*.

Waring, R.H. and Running, S. W., 2007. Forest ecosystems: analysis at multiple scales, 3rd edition, Elsevier. Amsterdam, The Netherlands.

Weiss, M., Baret, F., Smith, G. J., Jonckheere, I. and Coppin, P., 2004. Review of methods for in situ leaf area index (LAI) determination: Part II. Estimation of LAI, errors and sampling. *Agricultural and Forest Meteorology,* 121**,** 37-53.

Wilson, J. W., 1963. Estimation of foliage denseness and foliage angle by inclined point quadrats. *Australian Journal of Botany,* 11**,** 95-105.